Dionne E. Maessen,[1,2] Olaf Brouwers,[1,2] Katrien H. Gaens,[1,2] Kristiaan Wouters,[1,2] Jack P. Cleutjens,[1,3] Ben J. Janssen,[1,4] Toshio Miyata,[5] Coen D. Stehouwer,[1,2] and Casper G. Schalkwijk[1,2]

Delayed Intervention With Pyridoxamine Improves Metabolic Function and Prevents Adipose Tissue Inflammation and Insulin Resistance in High-Fat Diet–Induced Obese Mice

Diabetes 2016;65:956–966 | DOI: 10.2337/db15-1390

OBESITY STUDIES

Obesity is associated with an increased risk for the development of type 2 diabetes and vascular complications. Advanced glycation end products are increased in adipose tissue and have been associated with insulin resistance, vascular dysfunction, and inflammation of adipose tissue. Here, we report that delayed intervention with pyridoxamine (PM), a vitamin B6 analog that has been identified as an antiglycating agent, protected against high-fat diet (HFD)–induced body weight gain, hyperglycemia, and hypercholesterolemia, compared with mice that were not treated. In both HFD-induced and *db/db* obese mice, impaired glucose metabolism and insulin resistance were prevented by PM supplementation. PM inhibited the expansion of adipose tissue and adipocyte hypertrophy in mice. In addition, adipogenesis of murine 3T3-L1 and human Simpson-Golabi-Behmel Syndrome preadipocytes was dose- and time-dependently reduced by PM, as demonstrated by Oil Red O staining and reduced expression of adipogenic differentiation genes. No ectopic fat deposition was found in the liver of HFD mice. The high expression of proinflammatory genes in visceral adipose tissue of the HFD group was significantly attenuated by PM. Treatment with PM partially prevented HFD-induced mild vascular dysfunction. Altogether, these findings highlight the potential of PM to serve as an intervention strategy in obesity.

Obesity is characterized by the dysregulation of adipokine production (1), which predisposes obese individuals to the development of cardiovascular and metabolic complications. Recently, we and others demonstrated the accumulation of advanced glycation end products (AGEs) in adipose tissue (2,3), and identified that they play an important role in obesity-induced insulin resistance and dysregulation of the expression of adipokines, such as interleukin (IL)-6 and adiponectin (2,4,5). AGEs are a heterogeneous family of nonenzymatically, post-translationally modified proteins and can be formed rapidly by the intracellular α-dicarbonyl compounds methylglyoxal (MGO), glyoxal (GO), and 3-deoxyglucosone (3-DG) (6). Because of the harmful effects elicited by AGEs, several inhibitors have been designed to inhibit their formation (7).

Currently, pyridoxamine (PM) is receiving considerable attention as a highly potent AGE inhibitor. PM, a vitamin B6 analog, has been identified as an antiglycating agent (8), possibly through the trapping of α-dicarbonyl compounds (9). Previous data have shown that PM inhibits AGE formation and retards the development of diabetic nephropathy and retinopathy in animal models of diabetes (10). Two trials (11,12) in patients with diabetic nephropathy demonstrated no adverse effects of PM and, thus, a favorable safety profile.

[1]CARIM School for Cardiovascular Diseases, Maastricht University Medical Center, Maastricht, the Netherlands
[2]Department of Internal Medicine, Maastricht University Medical Center, Maastricht, the Netherlands
[3]Department of Pathology, Maastricht University Medical Center, Maastricht, the Netherlands
[4]Department of Pharmacology, Maastricht University Medical Center, Maastricht, the Netherlands
[5]United Centers for Advanced Research and Translational Medicine, Tohoku University, Sendai, Japan

Corresponding author: Casper G. Schalkwijk, c.schalkwijk@maastrichtuniversity.nl.

Received 6 October 2015 and accepted 17 December 2015.

This article contains Supplementary Data online at http://diabetes.diabetesjournals.org/lookup/suppl/doi:10.2337/db15-1390/-/DC1.

Because of the accumulation of AGEs in obese adipose tissue and the link with insulin resistance and vascular complications, we postulate that inhibiting AGE formation will improve the metabolic and vascular profile in obesity. In the current study, we examine the effect of a delayed PM intervention on metabolic and vascular function in high-fat diet (HFD)–induced obese mice. By delaying PM treatment until 6 weeks after the start of HFD feeding, we mimic the clinical situation of obesity in which metabolic dysfunction has already developed. This delayed intervention enables us to investigate the capacity of PM to treat obesity-associated complications, rather than to prevent them.

RESEARCH DESIGN AND METHODS

Animals

Male C57BL/6J mice were purchased from The Jackson Laboratory (Charles River) and were maintained in a temperature-controlled room on a 12-h light-dark cycle. They were housed with two to three mice per cage and had free access to food and drinking water. After a 6-week run-in period eating a low-fat diet (LFD; 10% fat; catalog #D12450H; Research Diets), 12-week-old mice were divided into three groups. The LFD group (n = 15) continued on the same diet, whereas the other two groups (n = 15 per group) switched to the HFD (45% kcal% fat; catalog #D12451; Research Diets). After 6 weeks of being fed an HFD, one group started to receive PM (2 g/L) in the drinking water (HFD + PM), and 18 weeks later all mice were killed by means of CO_2 inhalation and subsequent exsanguination by cardiac puncture.

Male *db/db* mice were also purchased from The Jackson Laboratory (Charles River) and were included in the study at 6 weeks of age. They were treated with PM in their drinking water for 18 weeks. The *db/db* mice were housed and killed in the same way as described for the LFD- and HFD-fed C57BL/6J mice.

The experimental protocol was approved by the institutional Animal Experiments Committee of Maastricht University, and all experiments were performed by licensed users according to international guidelines. PM was provided by T. Miyata (Tohoku University, Sendai, Japan).

In Vivo Glucose Tolerance and Insulin Tolerance Tests

Intraperitoneal glucose tolerance tests (IPGTTs) were performed in all mice 13 weeks after the start of the study. After a 16-h overnight fasting period, whole-blood glucose was measured with a glucometer (Contour; Bayer, Leverkusen, Germany). After intraperitoneal glucose injection (2.0 g/kg body wt; Sigma-Aldrich, St. Louis, MO), blood glucose levels were measured at 15, 30, 60, 90, and 120 min. One week later, intraperitoneal insulin tolerance tests (IPITTs) were performed. To this end, mice were fasted for 4 h, and insulin was injected intraperitoneally at a dose of 0.5 units/kg body wt (Actrapid Penfill; Novo Nordisk, Bagsværd, Denmark). Blood samples were taken at the same time points as during the IPGTT, and blood glucose levels were assessed. In addition, the IPGTT and IPITT were also performed in *db/db* mice.

Biochemical Characterization

Fasted plasma total cholesterol and liver triglyceride levels were determined with enzymatic colorimetric tests using CHOD-PAP and GPO-PAP reagents, respectively (Instruchemie, Delfszijl, the Netherlands). Fasted plasma insulin and leptin levels were measured in a multiplexed sandwich immunoassay (K15124-C; Meso Scale Discovery, Rockville, MD). Plasma biomarkers were measured with a 7-plex multiarray biomarker assay (K15012-C; Meso Scale Discovery). The α-dicarbonyls MGO, GO, and 3-DG were measured using ultra-performance liquid chromatography tandem mass spectrometry (Waters, Milford, MA), as described previously (13).

Glyoxalase 1 (GLO1) activity was measured in protein lysates of visceral adipose tissue (VAT), according to the method of McLellan et al. (14). In short, GLO1 activity was assayed by spectrophotometry (Synergy; BioTek, Winooski, VT), by measuring the increase in absorbance at 240 nm as a result of the formation of *S*-D-lactoylglutathione for 20 min.

Immunohistochemical Tissue Characterization

During dissection of the mice, visceral, epididymal fat depots, and livers were isolated, weighed, and stored for further analyses. After overnight fixation in 4% formaldehyde, tissues were embedded in paraffin, and 4-μm sections were collected and stained with hematoxylin-eosin (H-E). Digital images were taken at a magnification of ×20 using a Leica DFC320 digital camera (Leica Microsystems, Wetzlar, Germany). Adipocyte cell size and cell diameter were quantified with morphometric analysis software (Leica QWin V3; Leica Microsystems, Wetzlar, Germany). Macrophage infiltration in VAT was scored based on the presence of crown-like structures with the following scores: 0, no crown-like structures; 1, 1 or 2 crown-like structures; 2, 3–9 crown-like structures; 3, 10–20 crown-like structures; and 4, >20 crown-like structures. The fat content of the liver was scored based on the presence of fat droplets with the following scores: 0, no fat droplets; 1, very few fat droplets; 2, few fat droplets; 3, multiple fat droplets; and 4, many fat droplets.

Preadipocyte Culture and Differentiation

Murine 3T3-L1 and human Simpson-Golabi-Behmel Syndrome (SGBS) preadipocytes were cultured and differentiated into adipocytes according to the appropriate protocol. In short, murine 3T3-L1 preadipocytes were maintained in DMEM high glucose (25 mmol/L) containing 10% FCS and 1% glutamine-penicillin/streptozotocin. After reaching 80% confluency, differentiation was induced with the standard culture medium supplemented with 0.5 mmol/L 3-isobutyl-1-methylxanthine, 10 μg/mL insulin, and 0.444 μg/mL dexamethasone. After 2 days, the first adipogenic differentiation medium was substituted by the standard culture

medium supplemented with 2.5 μg/mL insulin until day 12. Human SGBS preadipocytes were maintained in DMEM/HAM F12 culture medium supplemented with 10% FCS, 8 μg/mL biotin, 4 μg/mL pantothenate, and 1% glutamine-penicillin/streptozotocin; and were grown to confluence. Adipogenic differentiation was induced by incubating preadipocytes with serum-free culture medium containing 10 μg/mL human transferrin, 20 nmol/L insulin, 100 nmol/L cortisol, and 0.2 nmol/L triiodothyronine for 12 days. After 6 days of differentiation, this adipogenic differentiation medium was additionally supplemented with 25 nmol/L dexamethasone, 500 μmol/L 3-isobutyl-1-methylxanthine, and 2 μmol/L rosiglitazone (GlaxoSmithKline, London, U.K.). For both SGBS and 3T3-L1 cells, media were refreshed every other day. In addition to the normal differentiation condition, cells were also differentiated in the presence of 2 and/or 5 mmol/L PM. RNA was extracted from cells at day 0, 2, 5, and 7. Oil Red O staining (Sigma-Aldrich) and triglyceride measurements of both 3T3-L1 and SGBS cells during differentiation were performed following the manufacturer instructions to determine adiposity. Cell count was determined using a Bürker-Türk counting chamber.

Real-Time PCR

Total RNA was extracted from cells and VAT using TRIzol (Invitrogen, Bleiswijk, the Netherlands), and was reverse transcribed with the iScript cDNA Synthesis Kit (Bio-Rad, Veenendaal, the Netherlands). The expression of target genes was measured quantitatively by real-time PCR using SYBR Green mix (Bioline, London, U.K.). All primer sets used are listed in Supplementary Table 1. mRNA expression levels were normalized to two reference genes (cyclophilin A and β_2-microglobulin), and data were analyzed with the ΔCT method. Data are expressed as normalized gene expression levels relative to control.

Assessment of Cardiac Function, Vascular Stiffness, Blood Pressure, and Vascular Function

Cardiac dimensions and function were assessed under 2–3% isoflurane anesthesia. Briefly, echocardiographic recordings were made in parasternal long axis using a Vevo2100 Imaging Platform (Visual Sonics, Toronto, ON, Canada). Data were derived from left ventricular (LV) images in end-diastole and peak systole, and average values over at least three different cycles were used for analyses. Stroke volume was calculated from subtracting peak systolic LV values from end-diastolic LV values and multiplying them by heart rate to obtain cardiac output. Pulse wave velocity (PWV) was assessed using the Vevo2100 Ultrasound Machine. By visualizing the aortic arch, we measured the time frame of the forward wave (electrocardiogram triggered) between two aortic points and calculated the PWV.

In a subset of mice, blood pressure was measured under isoflurane anesthesia by the insertion of a PE-10 catheter in the abdominal aorta via the femoral artery and connected to a pressure transducer (Miller Instruments, Houston, TX). The pressure signal was digitally sampled at 2 kHz, and systolic and diastolic blood pressures were calculated over a 10- to 15-min time period after the stabilization of hemodynamic variables.

After careful dissection of the aorta, an aortic segment of the descending thoracic aorta was excised just above the diaphragm. These segments were then mounted in a myograph organ bath (model 610M; Danish Myo Technology, Aarhus, Denmark) with two steel 40-μm wires inserted through the lumen of the segments. The organ bath contained fresh Krebs-Ringer bicarbonate solution, consisting of 118 mmol/L NaCl, 4.7 mmol/L KCl, 1.2 mmol/L KH_2PO_4, 25 mmol/L $NaHCO_3$, 1.1 mmol/L $MgSO_4$, 2.5 mmol/L $CaCl_2$, and 5.0 mmol/L glucose, was maintained at 37°C and was gassed continuously with 95% O_2 and 5% CO_2 (pH 7.4). The internal diameter of each aorta was normalized by stretching the vessel to a diameter that yielded a wall tension equivalent to a transmural pressure of 100 mmHg. The isometric tension generated by the vessels was recorded using Powerlab 4/25 (ADInstruments, Oxford, U.K.), connected to the Myo interface. Maximum contraction was measured by incubation with 125 mmol/L K^+ plus 10 μmol/L phenylephrine (Sigma-Aldrich). Endothelium-independent vasorelaxation was tested with cumulative concentrations of acetylcholine (ACh; 0.001–10 μmol/L; Sigma-Aldrich) during contraction, induced by 10 μmol/L phenylephrine, with preincubation of 10 μmol/L indomethacin (Sigma-Aldrich) to block the synthesis of prostaglandins, and 100 μmol/L L-NG-nitro-L-arginine methyl ester (Sigma-Aldrich) to block endothelial nitric oxide synthase.

Statistical Analyses

All data are presented as the mean ± SEM. Statistical analyses were performed with SPSS Statistics Software, version 20 (IBM Corporation, Armonk, NY). One-way ANOVA was used to compare continuous variables between groups. Two-way repeated-measures ANOVA was used to compare groups or conditions over time. A P value of less than 0.05 was considered statistically significant.

RESULTS

Delayed Intervention With PM Prevents Body Weight Gain and Improves Metabolic Characteristics in HFD-Induced Obese Mice

Six weeks of HFD feeding resulted in significantly increased body weight, and plasma glucose and total cholesterol levels compared with LFD control mice (Table 1). Water intake and urine production were not altered as a result of the HFD. Thus, when we started PM intervention after the first 6 weeks, the metabolic function of the HFD mice was already impaired.

Metabolic characteristics of the mice at the end of the study are shown in Fig. 1. The administration of PM to the drinking water for 18 weeks inhibited body weight gain in HFD mice (Fig. 1*A* and *B*), despite equal calorie intake (Fig. 1*C*). In addition, we observed a trend toward metabolic improvement by PM supplementation for plasma glucose and cholesterol (Fig. 1*D* and *E*), whereas

Table 1—Characteristics of the mice before intervention with PM

Variable	LFD	HFD
Body weight (g)	25.3 ± 0.3	28.2 ± 0.4***
Calorie intake (kcal/day)	9.9 ± 0.2	11.1 ± 0.3**
Fasting plasma glucose (mmol/L)	8.0 ± 0.4	10.5 ± 0.4***
Fasting total cholesterol (mmol/L)	1.8 ± 0.1	2.4 ± 0.1***
Water intake (mL/day)	2.5 ± 0.1	2.6 ± 0.04
Urine production (μL/day)	456 ± 134	659 ± 90

Data represent the mean ± SEM. N = 15 and 30 mice for LFD and HFD, respectively. ***$P < 0.001$ compared with LFD. **$P < 0.01$ compared with LFD.

plasma insulin and leptin levels were significantly reduced by PM treatment in HFD-fed mice (Fig. 1*F* and *G*). There were no differences in water intake and urine production between the HFD and HFD + PM groups (data not shown).

Glucose Tolerance and Insulin Sensitivity Are Improved by PM in Both HFD-Induced and *db/db* Obese Mice

We further studied the effect of PM on metabolic function with both an IPGTT and an IPITT after 13 weeks of PM treatment. The results of the IPGTT demonstrated that HFD mice had significantly lower glucose tolerance than LFD mice, which was improved by PM (Fig. 2*A*). After insulin injection, we found an impaired decline in glucose in the HFD group compared with the LFD group with an attenuation of this impairment by PM (Fig. 2*B*). These results demonstrate that treatment with PM is associated with general improvement in glucose tolerance and insulin sensitivity. We also performed the IPGTT and IPITT in obese *db/db* mice that had and had not been treated with PM. In line with our data from the HFD mice, PM administration also improved both glucose tolerance (Fig. 2*C*) and insulin sensitivity (Fig. 2*D*) in *db/db* mice.

PM Prevents Adipose Tissue Expansion and Hypertrophy by Inhibiting Adipogenesis

Histochemistry demonstrated enlarged adipocytes in the VAT of HFD mice compared with LFD mice (Fig. 3*A*). Morphometric analysis demonstrated an increased cell size and adipocyte diameter in the HFD group compared with the LFD control group (Fig. 3*B* and *C*). Both the HFD-induced increase in adipocyte diameter and cell size were attenuated by PM. In addition, the HFD-induced increase in the mass of VAT was attenuated by PM (Fig. 3*D*). To investigate the potential of PM to inhibit glycation in VAT, we assessed the levels of the α-dicarbonyls

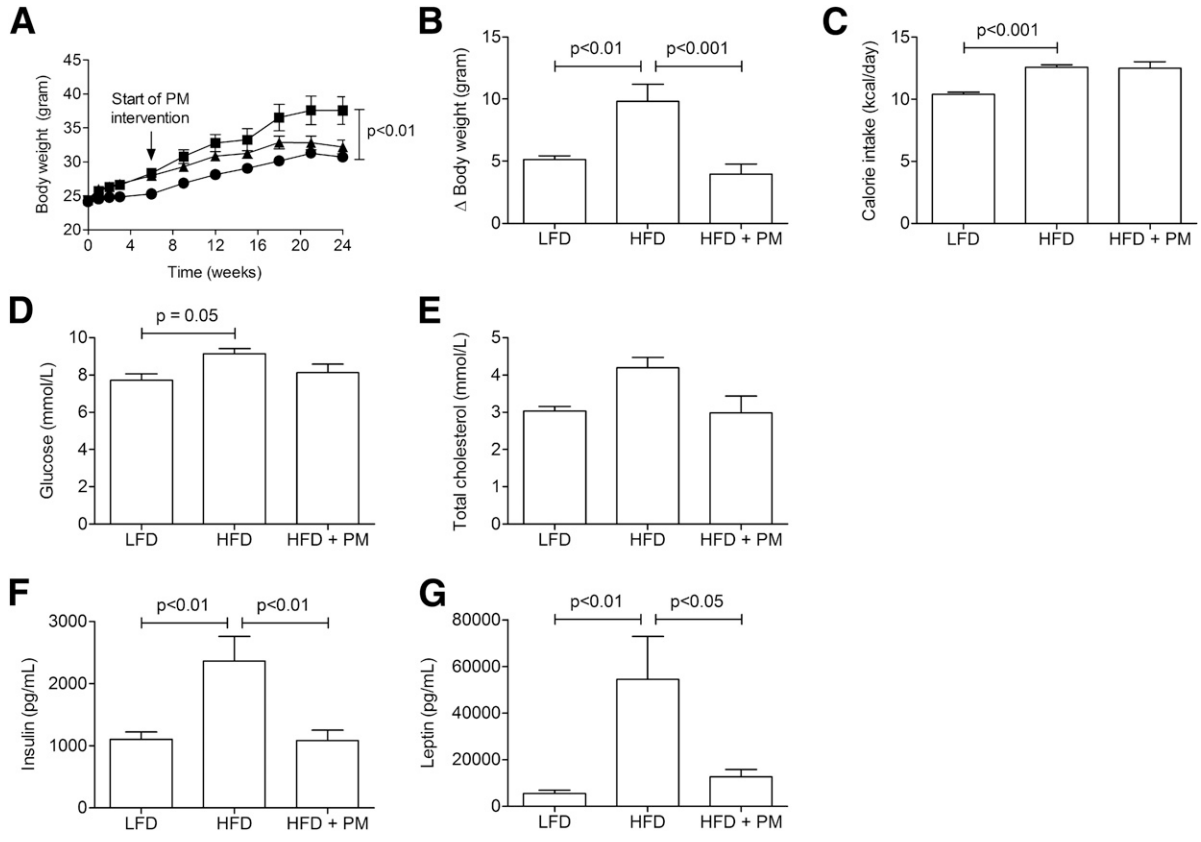

Figure 1—Metabolic parameters of the mice at the end of the study. *A*: Progress of body weight over time. *B*: Body weight gain during the study. *C*: Average calorie intake during the study. Fasting plasma glucose (*D*), cholesterol (*E*), insulin (*F*), and leptin (*G*) levels. Data represent the mean ± SEM. N = 11–15 mice per group. Circles, LFD; squares, HFD; triangles, HFD + PM.

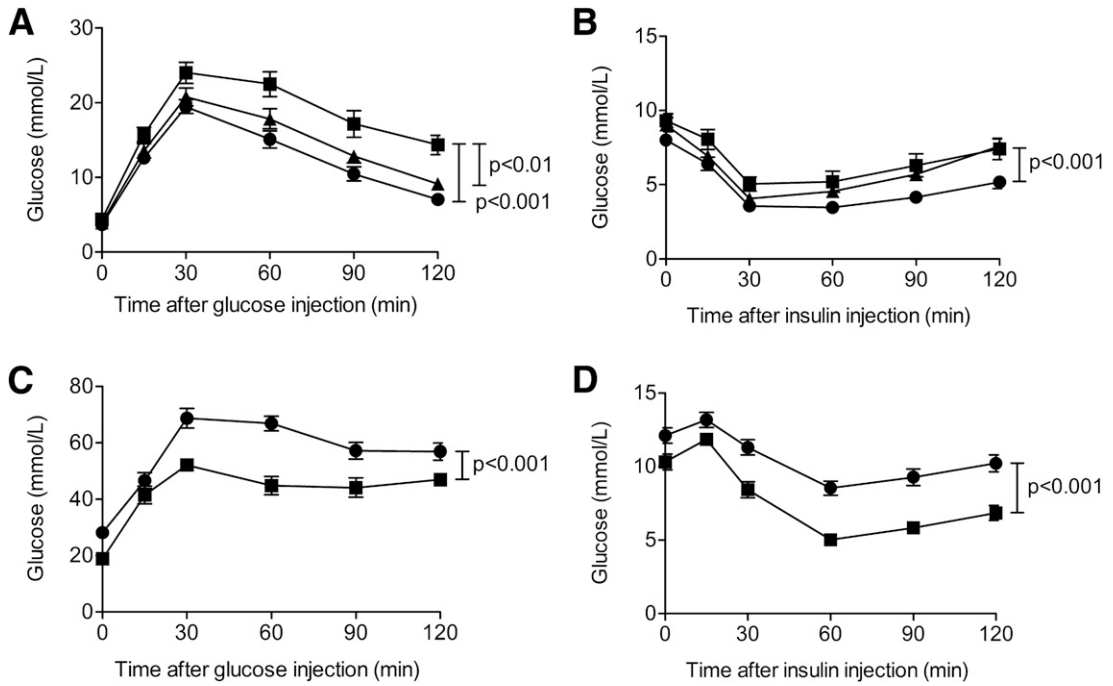

Figure 2—PM prevents insulin resistance in HFD-induced and *db/db* obese mice. Glucose homeostasis was assessed by an IPGTT (*A*) and an IPITT (*B*) in LFD mice, HFD mice, and HFD + PM mice. The IPGTT (*C*) and IPITT (*D*) were also performed in *db/db* mice, either treated or not treated with PM. Data represent the mean ± SEM. For *A* and *B*: circles, LFD; squares, HFD; triangles, HFD + PM. For *C* and *D*: circles, *db/db*; squares, *db/db* + PM. For *A* and *B*, n = 13–15 mice per group. For *C* and *D*, n = 7–15 mice per group.

MGO, GO, and 3-DG (Fig. 3*E–G*). We observed a trend toward increased α-dicarbonyl levels in VAT of the HFD group, which was reduced by PM. The activity of GLO1, the major enzyme for the detoxification of α-dicarbonyls, was reduced in VAT in the HFD group, although it was not statistically significant, and was improved by PM (Fig. 3*H*). The α-dicarbonyl levels, as well as GLO-1 activity, did not differ between LFD and HFD in the subcutaneous adipose tissue (data not shown).

To elucidate the mechanism behind PM-induced improvements in adiposity, we used the following two in vitro models of adipogenesis: murine 3T3-L1 and human SGBS preadipocytes. Both cell lines were differentiated by the appropriate differentiation mix, in the presence or absence of 2 and/or 5 mmol/L PM. Pictures of 3T3-L1 adipocytes demonstrated that cells differentiated in the presence of 5 mmol/L PM contained fewer fat droplets compared with untreated adipocytes (Fig. 4*A*). The inhibition of adipogenesis by PM was confirmed by Oil Red O staining (Fig. 4*B*), triglyceride quantification (Fig. 4*C*), and quantitative analysis of the expression of the adipogenic markers peroxisome proliferator–activated receptor γ (PPARγ), CCAAT/enhancer-binding protein α (C/EBPα), SREBP-1C, fatty acid synthase (FASN), lipoprotein lipase (LPL), and CD36 (Fig. 4*D–I*). Gene expression levels of SREBP cleavage-activating protein (SCAP) were unaffected by either HFD or PM (data not shown). Oil Red O staining and triglyceride quantification demonstrated a dose-dependent effect of PM on adipogenesis. These findings were all confirmed in human SGBS adipocytes (data not shown). We also investigated whether incubation with PM already had an effect on adipogenesis of 3T3-L1 cells in the first 2 days of the differentiation process, in which the preadipocytes still have the capacity to proliferate. To study this, 3T3-L1 preadipocytes were differentiated into adipocytes, and 5 mmol/L PM was added either from the start of the differentiation process (T = 0) or 2 days later (T = 2). We found that treatment with PM from T = 0 inhibited adipogenesis even more than when PM was added from T = 2, as reflected by Oil Red O absorbance and PPARγ mRNA expression (Supplementary Fig. 1*A* and *B*). Moreover, incubation with 5 mmol/L PM had no effect on the proliferation of the 3T3-L1 preadipocytes during the first 2 days of the differentiation process (Supplementary Fig. 1*C*).

Lipid Content in the Liver of HFD-Induced Obese Mice Is Reduced by PM

Because the liver often serves as an ectopic site of fat deposition, we investigated whether a reduction in adiposity by PM would lead to a flux of fat to the liver of HFD mice. H-E staining of liver sections demonstrated that livers of HFD mice contained more fat droplets (Fig. 5*A* and *B*). Treatment with PM in HFD mice resulted in fewer fat droplets in the liver. In line, triglyceride content was increased in the liver of HFD mice, but this was reduced by treatment with PM (Fig. 5*C*). Thus, a reduction in white adipose tissue by PM did not lead to ectopic fat deposition in the liver.

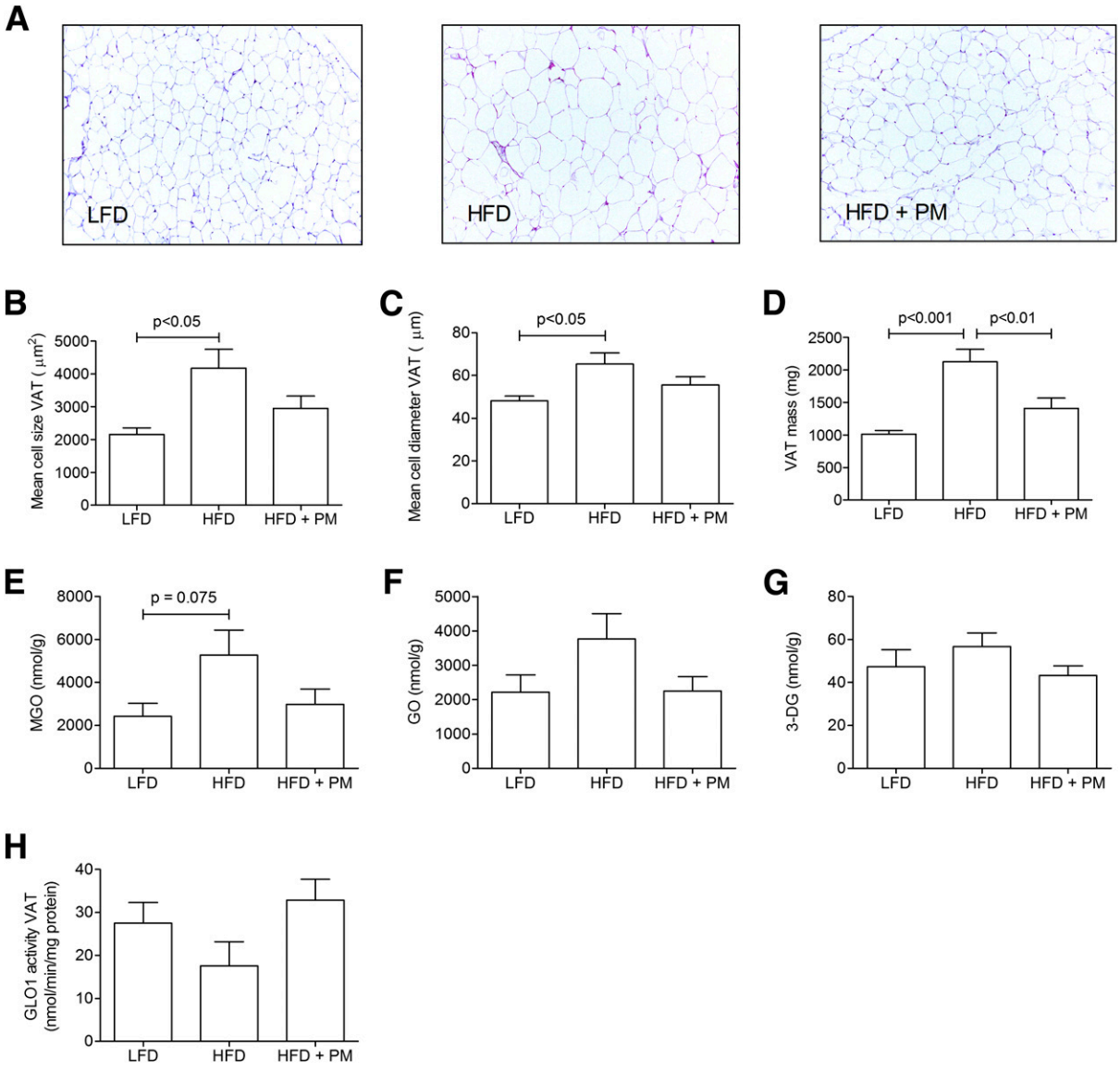

Figure 3—PM reduces obesity-related adiposity and partially prevents the formation of α-dicarbonyls in adipose tissue. *A*: Representative pictures of histochemical H-E staining of VAT, used for the quantification of cell size (*B*) and measurement of the diameter of individual adipocytes (*C*). *D*: Weight of visceral adipose mass. MGO (*E*), GO (*F*), and (*G*) 3-DG levels in VAT. *H*: Activity of the GLO1 enzyme in VAT. Data represent the mean ± SEM. *N* = 11–15 mice per group.

PM Prevents HFD-Induced Adipose Tissue Inflammation

To further examine the effect of PM on HFD-induced metabolic dysfunction in mice, we first characterized the VAT on the level of inflammation. Histochemical staining revealed an increased accumulation of macrophages in the VAT of HFD mice compared with that of LFD mice (Fig. 6*A* and *B*). The formation of these so-called crown-like structures was ameliorated by PM. Quantitative analyses of inflammatory gene expression levels demonstrated that HFD-induced gene expression levels of tumor necrosis factor-α (TNF-α), MCP-1, CD11c, and MHC-II, and HFD-induced reduction of adiponectin were attenuated by PM treatment (Fig. 6*C*–*G*). In plasma, however, we did not find any differences in the concentrations of interferon-γ, IL-1β, IL-10, IL-12, IL-2, IL-6, TNF-α, and mouse keratinocyte–derived chemokine between the groups (data not shown).

HFD-Induced Mild Vascular Dysfunction Is Partially Prevented by PM

ACh-induced, endothelium-independent vasorelaxation of mouse aortas was slightly impaired in HFD mice (Fig. 7*A*). This was improved when mice were treated with PM, although it was not statistically significant. The $\log EC_{50}$ (log half-maximal effective concentration) of ACh to

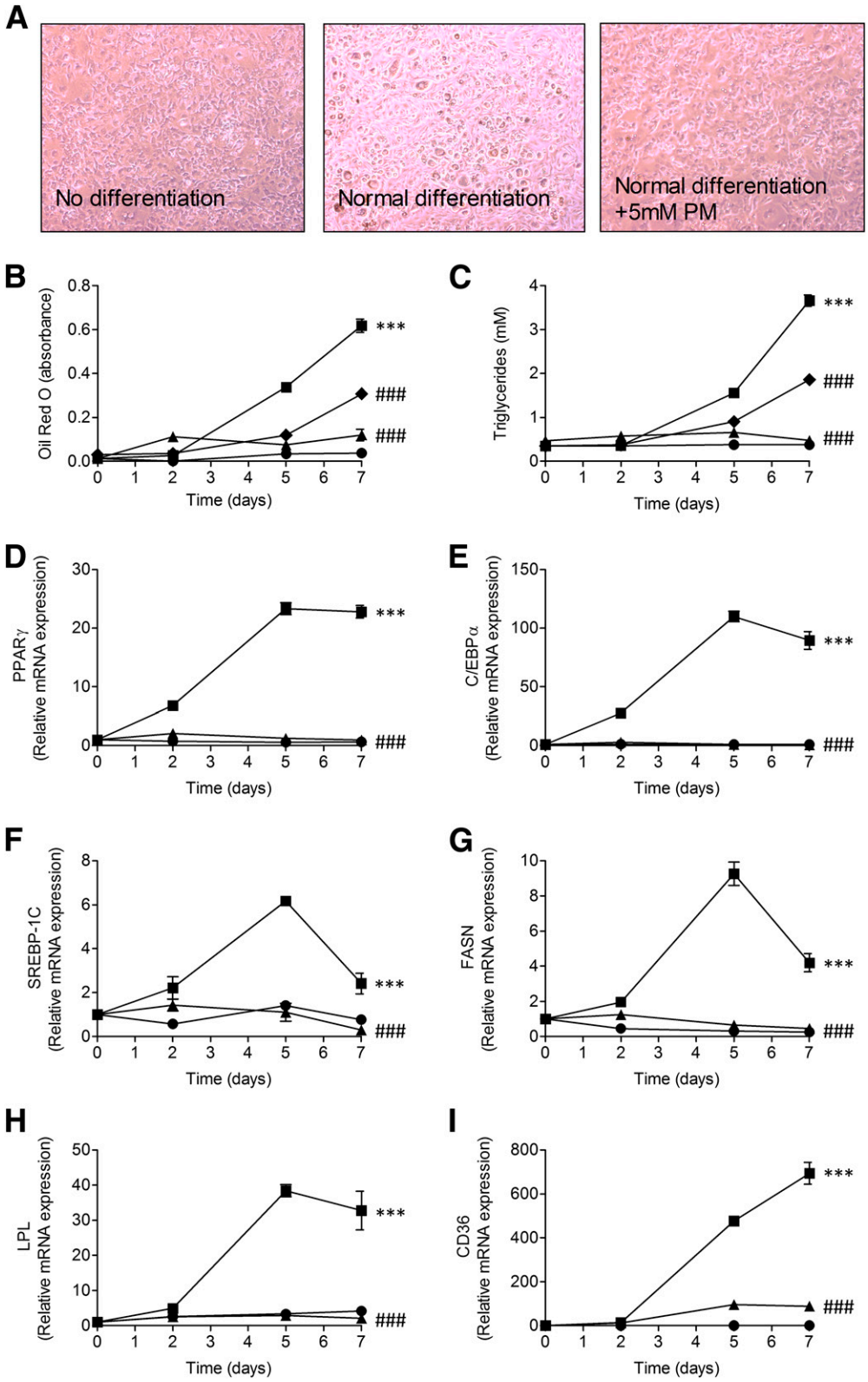

Figure 4— PM inhibits adipogenesis in vitro in a dose-dependent way. *A* and *B*: Oil Red O staining of differentiating 3T3-L1 adipocytes. *C*: Triglyceride content in 3T3-L1 adipocytes during 7 days of adipogenic differentiation. *D–I*: Gene expression levels of adipogenic markers in differentiating murine 3T3-L1 adipocytes. Data represent the mean ± SEM. ***$P < 0.001$, normal differentiation compared with no differentiation; ###$P < 0.001$, normal differentiation plus 2 or 5 mmol/L PM compared with normal differentiation. For *B* and *C*: circles, no differentiation; squares, normal differentiation; diamonds, normal differentiation plus 2 mmol/L PM; triangles, normal differentiation plus 5 mmol/L PM. For *D–I*: circles, no differentiation; squares, normal differentiation; triangles, normal differentiation plus 5 mmol/L PM.

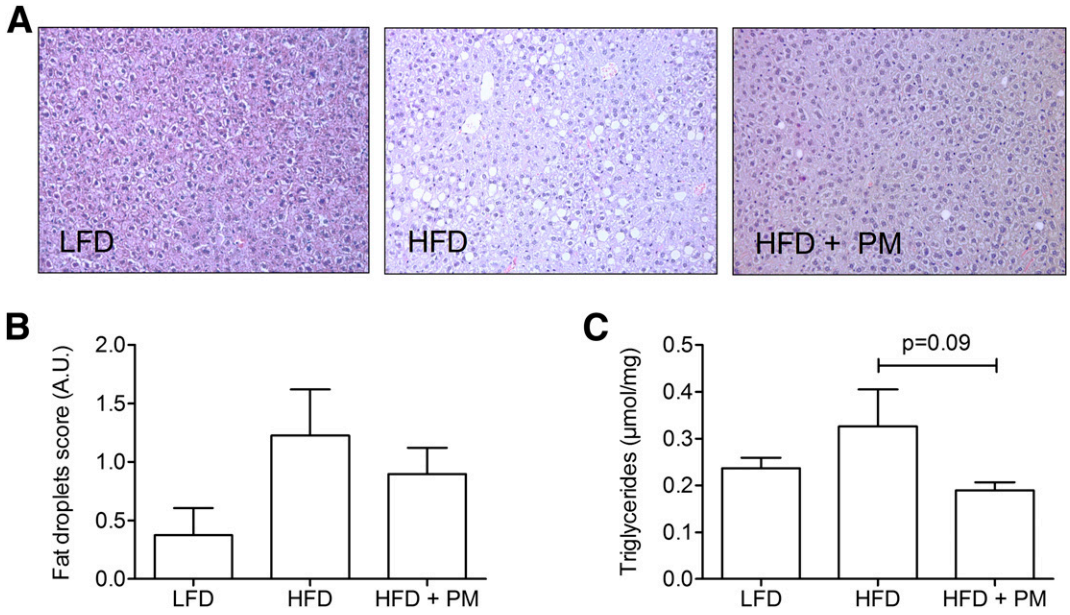

Figure 5—PM reduces HFD-induced moderate fat deposition in the liver. *A*: Representative pictures of H-E staining of the liver, showing fat droplets. *B*: Quantification of the liver fat droplets, as shown in *A*. *C*: Triglyceride content in the liver. Data represent the mean ± SEM. *N* = 11–15 mice per group. A.U., arbitrary units.

achieve 50% of the maximal vasorelaxation was reduced in the HFD group, which was prevented by PM (Fig. 7*B*). Neither HFD nor PM had an effect on other vascular parameters, including systolic blood pressure, diastolic blood pressure, heart rate, cardiac output, ejection fraction, and PWV (Supplementary Fig. 2).

DISCUSSION

In the current study, we investigated the effects of PM on obesity and its related complications. We have shown that obesity-associated metabolic dysfunction and complications in obese mice were ameliorated by a delayed intervention with PM. HFD-induced increases in body weight, hyperglycemia, hypercholesterolemia, and levels of leptin and insulin were all reduced by PM. In addition, PM is associated with a general increase in glucose tolerance and insulin sensitivity. Furthermore, the expansion of adipose tissue and hypertrophy of adipocytes in obese mice were inhibited by PM, most likely via the inhibition of adipogenesis. PM improved vasorelaxation of the aorta, but it had no observable effect on other vascular parameters.

By feeding mice an HFD, we induced a state of metabolic dysfunction, as indicated by an increase in body weight and severe hyperglycemia and hypercholesterolemia, and increased plasma levels of insulin and leptin. We have shown, in a delayed intervention study with PM, that PM was able to improve these metabolic dysfunctions, including reducing insulin resistance in both HFD mice and *db/db* mice.

The beneficial effect of PM on metabolic function was also reflected by a reduction of the VAT mass, most likely via the inhibition of adipogenesis. This concept was demonstrated in vitro by reduced Oil Red O staining and triglyceride content in differentiating murine 3T3-L1 and human SGBS cells. In addition, we found that PM limited the induction of important adipogenic differentiation genes such as PPARγ, C/EBPα, SREBP-1C, FASN, LPL, and CD36. SREBP-1C is a transcription factor that is known to induce the expression of adipogenic genes such as LPL and FASN, but it also induces PPARγ expression, which enhances adipogenic gene expression even more (15,16). As both SREBP-1C and PPARγ expression and the expression of their target genes are decreased, this suggests an inhibitory effect of PM on adipogenesis, possibly via the inhibition of SREBP-1C. In the literature, it has been described that the AGE N(ε)-(carboxymethyl) lysine (CML) interferes with the SCAP/SREBP-1C pathway (17,18). In our study, we did not find any effect of PM on mRNA expression levels of SCAP in adipocytes. However, in different cell types CML has been described to colocalize with SCAP (17–19), suggesting a considerable glycation of SCAP, and consequently leading to altered function of SCAP. Therefore, the glycation of SCAP, along with the possible direct effects of PM, may be a possible mechanism by which AGEs enhance adipogenesis. The dangerous reverse side of smaller fat depots in obesity is ectopic fat deposition. The most important organ that is known to be at risk for ectopic fat deposition is the liver. However, in this study, we demonstrated that the inhibition of adipogenesis by PM in HFD mice did not lead to fatty liver disease. On the contrary, PM treatment resulted in less fat content in HFD livers.

Obesity is associated with a dysregulated expression of adipocytokines (2,20). We and others (2,21,22) have

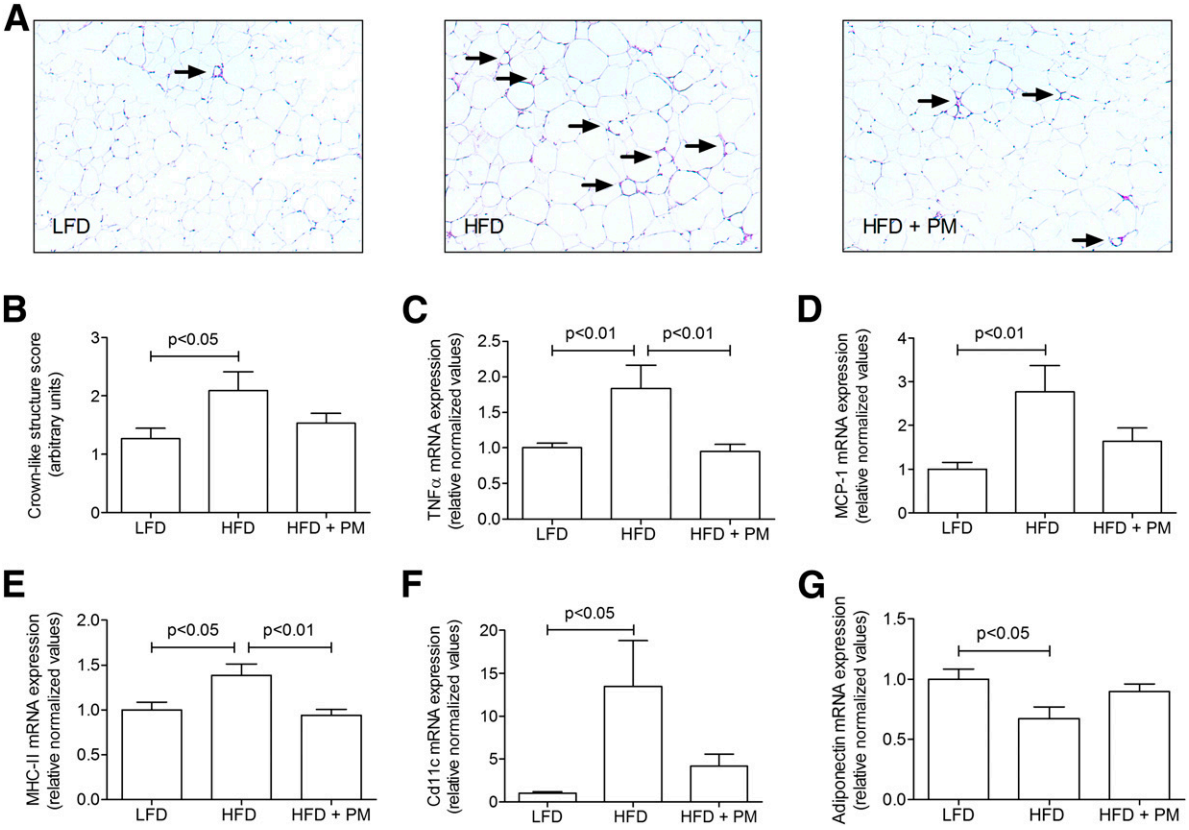

Figure 6—HFD-induced inflammation in VAT is prevented by PM. *A*: Representative pictures of H-E staining of VAT, showing crown-like structures. *B*: Quantification of crown-like structures, as shown in *A.* Quantitative PCR is used for the quantification of gene expression of the inflammatory markers TNF-α (*C*), MCP-1 (*D*), MHC-II (*E*), CD11c (*F*), and adiponectin (*G*). Data represent the mean ± SEM. *N* = 11–15 mice per group.

very recently demonstrated that AGEs are implicated herein. In the current study, the accumulation of macrophages, the so-called crown-like structures, and increased proinflammatory gene expression levels in VAT of HFD mice were observed, and the number of crown-like structures and the expression of proinflammatory cytokines TNF-α, MCP-1, CD11c, and MHC-II were strongly reduced by PM; whereas, the expression of the anti-inflammatory cytokine adiponectin was increased. Thus, supplementation with PM was associated with a normalization of the inflammatory phenotype of VAT in HFD mice. These results are in line with our previous work, in which we demonstrated that CML accumulation in adipose tissue of obese *db/db* mice was associated with a proinflammatory phenotype of the adipose tissue. When the receptor for AGEs was absent, inflammation levels were normalized (2). Together, these data

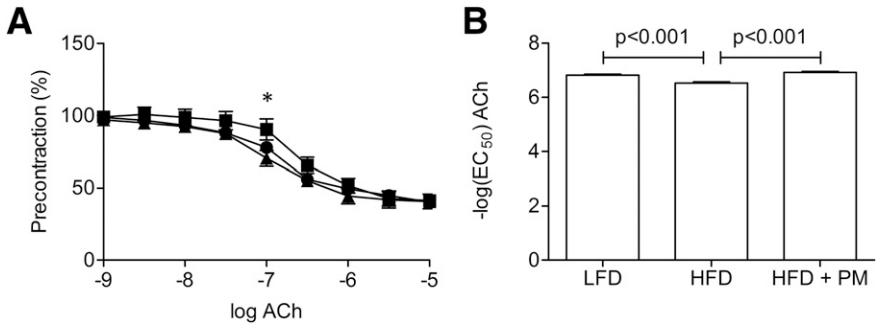

Figure 7—PM partially prevents mild HFD-induced vascular dysfunction. *A*: ACh-induced, endothelium-independent vasorelaxation of isolated aortas. *B*: $-\text{LogEC}_{50}$ of ACh in endothelium-independent vasorelaxation of the aorta. Data represent the mean ± SEM. *$P < 0.05$, HFD compared with LFD. *N* = 11–14 mice per group. Circles, LFD; squares, HFD; triangles, HFD + PM.

form a strong body of evidence that the accumulation of AGEs in adipose tissue plays a key role in the pathogenesis of adipose tissue inflammation.

In the VAT of HFD mice, we found a trend toward decreased GLO1 activity. Because inflammation reduces GLO1 activity (23), the proinflammatory phenotype of the VAT in HFD mice is most likely responsible for the reduction in GLO1 activity. In line with this, PM reduces adipose tissue inflammation and, thus, causes normalization of GLO1 activity in the VAT of HFD mice.

Some of our findings regarding PM have previously been described in comparable studies (24,25). However, in those studies, PM had been administered to mice from the start of the HFD, implying that metabolic function at the start of PM treatment was not comparable to that of obesity. Because we hypothesize that PM might be a potential treatment for obesity and its comorbidities, we mimicked the human situation by starting treatment with PM when obesity had already developed. To the best of our knowledge, our study is the first to use PM in such a delayed intervention.

Although AGEs have been described in relation to vascular complications (26), we only found an improvement in aortic vasorelaxation, while improvements in additional vascular parameters were lacking. These findings are in line with those of Hagiwara et al. (24), who similarly found no effect of PM on blood pressure in HFD-induced obese mice. In aged mice, however, it has been noted that PM prevents age-related aortic stiffening and vascular resistance in association with reduced collagen glycation (27). Because we did not see large effects of HFD on the development of serious (cardio)vascular complications within 24 weeks of HFD, age-related AGE accumulation may be more relevant for vascular complications than obesity-related AGE accumulation. It might be that our animals were not old enough to develop (cardio)vascular complications as a result of eating an HFD.

In clinical trials, treatment with PM has mainly been described in the setting of diabetic nephropathy. Several preclinical studies (28–32) in animal models of diabetic nephropathy have demonstrated that oral supplementation of PM is effective in preserving renal function. In a combined multicenter phase II trial involving patients with type 2 diabetes with overt nephropathy, PM was demonstrated to be generally safe and to have a potential effect in preserving diabetic kidney function (11). In contrast, a second clinical trial (12) reported no beneficial effect of PM in reducing creatinine levels, although it suggested that patients with less advanced renal impairment might benefit. A third clinical trial (33) addressed the efficacy and tolerability of PM in osteoarthritis. It reported no adverse effects after 6 months of PM treatment, while a combined treatment with PM significantly decreased AGEs, inflammation, and pain in patients with osteoarthritis.

In conclusion, we have demonstrated that a delayed intervention with PM is associated with improvement of several aspects of obesity, including metabolic dysfunction, insulin resistance, and adipose tissue inflammation. These findings indicate that PM may be a potential novel treatment for obesity-associated metabolic dysfunction and complications. A clinical trial with PM in obese individuals would elucidate the efficacy of PM in human obesity complications.

Acknowledgments. For expert technical assistance, the authors thank Marjo van de Waarenburg, Jean Scheijen, Margee Robertus, Vicky Vermeulen, and Sabine Daemen (all from the Department of Internal Medicine, Maastricht University Medical Center, Maastricht, the Netherlands); and Jacques Debets (Department of Pharmacology, Maastricht University Medical Center, Maastricht, the Netherlands).

Funding. The current study was funded by Top Institute Food and Nutrition, a public-private partnership on precompetitive research in food and nutrition.

The funders had no role in study design, data analysis, decision to publish, or preparation of the article.

Duality of Interest. No potential conflicts of interest relevant to this article were reported.

Author Contributions. D.E.M. researched the data, contributed to the discussion, and wrote and edited the article. O.B. and K.H.G. researched the data, contributed to the discussion, and reviewed and edited the article. K.W., C.D.S., and C.G.S. contributed to the discussion, and reviewed and edited the article. J.P.C. designed the computer program for quantitative analysis of the adipocytes, and reviewed and edited the article. B.J.J. provided equipment, supported the vascular measurements, and reviewed and edited the article. T.M. provided the pyridoxamine, and reviewed and edited the article. C.G.S. is the guarantor of this work and, as such, had full access to all the data in the study and takes responsibility for the integrity of the data and the accuracy of the data analysis.

References

1. Cao H. Adipocytokines in obesity and metabolic disease. J Endocrinol 2014; 220:T47–T59

2. Gaens KH, Goossens GH, Niessen PM, et al. Nε-(carboxymethyl)lysine-receptor for advanced glycation end product axis is a key modulator of obesity-induced dysregulation of adipokine expression and insulin resistance. Arterioscler Thromb Vasc Biol 2014;34:1199–1208

3. Song F, Hurtado del Pozo C, Rosario R, et al. RAGE regulates the metabolic and inflammatory response to high-fat feeding in mice. Diabetes 2014;63: 1948–1965

4. Schalkwijk CG, Brouwers O, Stehouwer CD. Modulation of insulin action by advanced glycation endproducts: a new player in the field. Horm Metab Res 2008;40:614–619

5. Sandu O, Song K, Cai W, Zheng F, Uribarri J, Vlassara H. Insulin resistance and type 2 diabetes in high-fat-fed mice are linked to high glycotoxin intake. Diabetes 2005;54:2314–2319

6. Thornalley PJ, Langborg A, Minhas HS. Formation of glyoxal, methylglyoxal and 3-deoxyglucosone in the glycation of proteins by glucose. Biochem J 1999; 344:109–116

7. Schalkwijk CG, Miyata T. Early- and advanced non-enzymatic glycation in diabetic vascular complications: the search for therapeutics. Amino Acids 2012; 42:1193–1204

8. Booth AA, Khalifah RG, Hudson BG. Thiamine pyrophosphate and pyridoxamine inhibit the formation of antigenic advanced glycation end-products: comparison with aminoguanidine. Biochem Biophys Res Commun 1996;220: 113–119

9. Voziyan PA, Hudson BG. Pyridoxamine as a multifunctional pharmaceutical: targeting pathogenic glycation and oxidative damage. Cell Mol Life Sci 2005;62: 1671–1681

10. Engelen L, Stehouwer CD, Schalkwijk CG. Current therapeutic interventions in the glycation pathway: evidence from clinical studies. Diabetes Obes Metab 2013;15:677–689

11. Williams ME, Bolton WK, Khalifah RG, Degenhardt TP, Schotzinger RJ, McGill JB. Effects of pyridoxamine in combined phase 2 studies of patients with type 1 and type 2 diabetes and overt nephropathy. Am J Nephrol 2007;27:605–614
12. Lewis EJ, Greene T, Spitalewiz S, et al.; Collaborative Study Group. Pyridorin in type 2 diabetic nephropathy. J Am Soc Nephrol 2012;23:131–136
13. Scheijen JL, Schalkwijk CG. Quantification of glyoxal, methylglyoxal and 3-deoxyglucosone in blood and plasma by ultra performance liquid chromatography tandem mass spectrometry: evaluation of blood specimen. Clin Chem Lab Med 2014;52:85–91
14. McLellan AC, Phillips SA, Thornalley PJ. The assay of S-D-lactoylglutathione in biological systems. Anal Biochem 1993;211:37–43
15. Kim JB, Spiegelman BM. ADD1/SREBP1 promotes adipocyte differentiation and gene expression linked to fatty acid metabolism. Genes Dev 1996;10: 1096–1107
16. Fajas L, Schoonjans K, Gelman L, et al. Regulation of peroxisome proliferator-activated receptor gamma expression by adipocyte differentiation and determination factor 1/sterol regulatory element binding protein 1: implications for adipocyte differentiation and metabolism. Mol Cell Biol 1999;19:5495–5503
17. Mastrocola R, Collino M, Nigro D, et al. Accumulation of advanced glycation end-products and activation of the SCAP/SREBP Lipogenetic pathway occur in diet-induced obese mouse skeletal muscle. PLoS One 2015;10:e0119587
18. Mastrocola R, Collino M, Rogazzo M, et al. Advanced glycation end products promote hepatosteatosis by interfering with SCAP-SREBP pathway in fructose-drinking mice. Am J Physiol Gastrointest Liver Physiol 2013;305:G398–G407
19. Yuan Y, Zhao L, Chen Y, et al. Advanced glycation end products (AGEs) increase human mesangial foam cell formation by increasing Golgi SCAP glycosylation in vitro. Am J Physiol Renal Physiol 2011;301:F236–F243
20. Leal VdeO, Mafra D. Adipokines in obesity. Clin Chim Acta 2013;419:87–94
21. Stirban A, Negrean M, Götting C, et al. Dietary advanced glycation end-products and oxidative stress: in vivo effects on endothelial function and adipokines. Ann N Y Acad Sci 2008;1126:276–279
22. Gaens KH, Stehouwer CD, Schalkwijk CG. Advanced glycation endproducts and its receptor for advanced glycation endproducts in obesity. Curr Opin Lipidol 2013;24:4–11
23. Hanssen NM, Wouters K, Huijberts MS, et al. Higher levels of advanced glycation endproducts in human carotid atherosclerotic plaques are associated with a rupture-prone phenotype. Eur Heart J 2014;35:1137–1146
24. Hagiwara S, Gohda T, Tanimoto M, et al. Effects of pyridoxamine (K-163) on glucose intolerance and obesity in high-fat diet C57BL/6J mice. Metabolism 2009;58:934–945
25. Unoki-Kubota H, Yamagishi S, Takeuchi M, Bujo H, Saito Y. Pyridoxamine, an inhibitor of advanced glycation end product (AGE) formation ameliorates insulin resistance in obese, type 2 diabetic mice. Protein Pept Lett 2010;17: 1177–1181
26. Stirban A, Gawlowski T, Roden M. Vascular effects of advanced glycation endproducts: clinical effects and molecular mechanisms. Mol Metab 2014;3:94–108
27. Wu ET, Liang JT, Wu MS, Chang KC. Pyridoxamine prevents age-related aortic stiffening and vascular resistance in association with reduced collagen glycation. Exp Gerontol 2011;46:482–488
28. Degenhardt TP, Alderson NL, Arrington DD, et al. Pyridoxamine inhibits early renal disease and dyslipidemia in the streptozotocin-diabetic rat. Kidney Int 2002; 61:939–950
29. Zhu P, Lin H, Sun C, et al. Synergistic effects of telmisartan and pyridoxamine on early renal damage in spontaneously hypertensive rats. Mol Med Rep 2012;5:655–662
30. Waanders F, van den Berg E, Nagai R, van Veen I, Navis G, van Goor H. Renoprotective effects of the AGE-inhibitor pyridoxamine in experimental chronic allograft nephropathy in rats. Nephrol Dial Transplant 2008;23:518–524
31. Alderson NL, Chachich ME, Youssef NN, et al. The AGE inhibitor pyridoxamine inhibits lipemia and development of renal and vascular disease in Zucker obese rats. Kidney Int 2003;63:2123–2133
32. Tanimoto M, Gohda T, Kaneko S, et al. Effect of pyridoxamine (K-163), an inhibitor of advanced glycation end products, on type 2 diabetic nephropathy in KK-A(y)/Ta mice. Metabolism 2007;56:160–167
33. Garg S, Syngle A, Vohra K. Efficacy and tolerability of advanced glycation end-products inhibitor in osteoarthritis: a randomized, double-blind, placebo-controlled study. Clin J Pain 2013;29:717–724